DOI 10.48612/fpg/4heu-kxbn-gg7t

Marine Hydrophysical Institute, Russian Academy of Sciences, 299011, Kapitanskaya Str., 2, Sevastopol, Russia
*E-mail: artam-ant@yandex.ru

THE RELATIONSHIP OF THE SPATIAL STRUCTURE OF THE TOTAL SUSPENDED MATTER CONCENTRATION AND HYDROLOGICAL PARAMETERS IN THE NORTHERN BLACK SEA ACCORDING TO CONTACT MEASUREMENTS

Received 14.01.2022, Revised 20.04.2022, Accepted 26.04.2022

Abstract

Here we describe the features of the horizontal and vertical distribution of total suspended matter in the northern part of the Black Sea and their relationships with the water temperature, salinity, and density fields measured at the identical grid during hydro-optical surveys from 2016 to 2020. The results show that the primary sources of increased total suspended matter concentrations in the northern part of the Black Sea are low-salinity and turbid waters of the Kerch Strait; runoffs of the Rioni, Enguri, and other rivers in the east of the survey area; together with freshened waters of the Dnieper, Dniester, and Danube runoff from the northwestern shelf. Higher turbidity was observed in the deep-water part of the sea, associated with the cyclonic gyres and meanders of the Rim Current effects. The total suspended matter vertical structure features an upper mixed layer, which usually coincides in thickness with the upper thermohaline upper mixed layer. Significant negative correlations were found for this layer comparing total suspended matter concentration versus temperature and salinity, while the correlation appears positive with density values. Below, a total suspended matter subsurface maximum was observed in the seasonal thermocline and pycnocline layer. The high turbidity layer appeared almost an order of magnitude thinner in the regions of maximum temperature gradients versus the areas where the temperature gradient was weak. A local total suspended matter minimum occurred below the cold intermediate core, corresponding to the main thermocline, halocline, and pycnocline layer. Beneath this minimum, there was a local increase of total suspended matter coinciding with the upper boundary of the hydrogen sulfide zone.

Keywords: total suspended matter, Black Sea, Rim Current, water temperature, salinity, density, circulation, upper mixed layer, thermocline, pycnocline, halocline

Морской гидрофизический институт РАН, 299011, Россия, г. Севастополь, ул. Капитанская, 2
*E-mail: artam-ant@yandex.ru

СВЯЗЬ ПРОСТРАНСТВЕННОЙ СТРУКТУРЫ КОНЦЕНТРАЦИИ ОБЩЕГО ВЗВЕШЕННОГО ВЕЩЕСТВА И ГИДРОЛОГИЧЕСКИХ ПАРАМЕТРОВ В СЕВЕРНОЙ ЧАСТИ ЧЕРНОГО МОРЯ ПО ДАННЫМ КОНТАКТНЫХ ИЗМЕРЕНИЙ

Статья поступила в редакцию 14.01.2022, после доработки 20.04.2022, принята в печать 26.04.2022

Аннотация

По данным гидрооптических съемок, выполненных в северной части Черного моря по одной и той же сетке в период с 2016 по 2020 гг., уточнены особенности горизонтальной и вертикальной структуры поля общего взвешенного вещества и оценена их связь с распределениями полей температуры воды, солености и плотности. Показано, что основными источниками повышенной концентрации общего взвешенного вещества в поверхностном слое северной части Черного моря являются низкосоленые и мутные воды, поступающие из Керченского пролива, воды стоков Риони, Ингури и других рек на востоке акватории и распресненные воды

Ссылка для цитирования: *Латушкин А.А.*, *Артамонов Ю.В.*, *Скрипалева Е.А.*, *Федирко А.В.* Связь пространственной структуры концентрации общего взвешенного вещества и гидрологических параметров в северной части Черного моря по данным контактных измерений // Фундаментальная и прикладная гидрофизика. 2022. Т. 15, № 2. С. 124–137. doi:10.48612/fpg/4heu-kxbn-gg7t

For citation: *Latushkin A.A.*, *Artamonov Yu.V.*, *Skripaleva E.A.*, *Fedirko A.V.* The Relationship of the Spatial Structure of the Total Suspended Matter Concentration and Hydrological Parameters in the Northern Black Sea According to Contact Measurements. *Fundamental and Applied Hydrophysics*. 2022, 15, 2, 124–137. doi:10.48612/fpg/4heu-kxbn-gg7t

Днепра, Днестра и Дуная, проникающие на акваторию съемок с северо-западного шельфа. В глубоководной части моря могут прослеживаться локальные области мутных вод, возникновение которых связано с особенностями вертикальной циркуляции в зонах циклонических круговоротов и меандров Основного Черноморского Течения. Вертикальная структура концентрации общего взвешенного вещества характеризовалась верхним квазиоднородным слоем, обычно совпадающим по толщине с верхним квазиоднородным слоем в полях термохалинных параметров. В пределах этого слоя между значениями концентрации общего взвешенного вещества и значениями температуры и солености наблюдалась значимая линейная отрицательная корреляция и значениями плотности — положительная. Глубже, в слое сезонных термоклина и пикноклина, прослеживался подповерхностный максимум концентрации общего взвешенного вещества. В областях, где наблюдался максимальный вертикальный градиент температуры, толщина слоя повышенной мутности уменьшалась почти на порядок по сравнению с районами, где градиент температуры был слабо выражен. Ниже ядра холодного промежуточного слоя в слое основных термоклина, галоклина и пикноклина прослеживался промежуточный минимум концентрации общего взвешенного вещества. Под этим минимумом располагался еще один слой повышенных значений концентрации общего взвешенного вещества, глубина которого совпадала с глубиной верхней границы сероводородной зоны.

Ключевые слова: общее взвешенное вещество, Черное море, Основное Черноморское Течение, температура воды, соленость, плотность, циркуляция, верхний квазиоднородный слой, термоклин, пикноклин, галоклин

1. Introduction

The intensive development of the shelf, the rapid growth of coastal cities and resort facilities, and the massive coastal development lead to a significant increase in the anthropogenic impact on the Black Sea ecosystem [1–3]. Along with river runoff, various industrial, agricultural, and domestic pollutants enter the sea. In this regard, the relevance of assessing the ecological state of the Black Sea waters, which is reflected in their hydro-optical structure, increases. The suspended matter has a significant effect on the formation of the latter [4–6], the indicator of the content of which is the light beam attenuation coefficient (BAC) [7–12].

At present, four main layers are distinguished in the vertical distribution of BAC in the deep part of the sea: surface, intermediate, boundary, and deep [7, 12]. The surface layer occupies the photic zone of the sea. Its lower boundary varies within 40–70 m on average. In summer, the surface layer is characterized by several BAC maxima, with the strongest maxima observed in the seasonal thermocline and in the upper part of the main halocline [7]. In the shelf part of the sea, in the vertical distribution, there is usually one BAC maximum [12]. In winter in the deep regions, only one BAC maximum persists in the vertical distribution due to the absence of a seasonal thermocline. In the shelf zone, the BAC distribution is vertically homogeneous [7, 12].

The intermediate layer is located at about 50–150m and is highly transparent. Its thickness in summer does not exceed 30 m; in winter, it can increase up to 80 m. High transparency is associated with the absence of organic matter accumulation conditions [7, 12]. Below lies the region of the oxygen zone transition into the hydrogen sulfide zone (suboxic redox zone [13]). Here, elevated turbidity is associated with a high content of suspended particles, including 93 % of inorganic and 7 % of organic particles [7, 14–18]. In the deep layer that starts at the upper boundary of the hydrogen sulfide zone, BAC increases monotonically with depth in the short-wave(violet) region of the spectrum, while the long-wave BAC remains constant vertically [14–20]. A possible explanation is given in [20]. Absorption by yellow matter, a part of organic compounds, is intense in the short-wave part of the spectrum and decreases sharply with the wavelength increase. Thus, it has a negligible effect on BAC in the long-wave part of the spectrum.

Studies of the horizontal distribution of transparency features showed that the most turbid waters appear in the surface layer on the northwestern shelf, which is associated with intense river runoff [7, 9–12, 21, 22]. Horizontal fields of hydro-optical parameters presented synoptic variability in the form of alternating areas of more transparent and relatively turbid waters, while the scale of synoptic formations was 10–100 km [12, 22].

Until recently, the general understanding of the Black Sea hydro-optical structure variability, especially in its deep-water part, is based on episodic measurements in different regions, seasons, and years, which makes it difficult to identify patterns of variability of hydro-optical fields on various spatiotemporal scales. In addition, to interpret the distributions of hydro-optical parameters, quasi-synchronous measurements of thermohaline characteristics and instrumental measurements of currents are required. Such

measurements have been regularly carried out since 2016 in the northern part of the Black Sea on the R/V *Professor Vodyanitsky*. Some results of these studies for individual surveys are reflected in [23–28]. In this paper, based on the generalization of all measurements performed from 2016 to 2020, we analyze the relationship between the spatial structure of the concentration of total suspended matter (TSM) with the distributions of hydrological parameters and water circulation. Note that in this study, the concentration of TSM refers to the concentration of all suspended particles that remain on the filter when using one or another filtration method.

2. Materials and methods

Hydro-optical and hydrological studies were carried out on the R/V *Professor Vodyanitsky* following the same scheme of stations in the northern part of the Black Sea from Cape Tarkhankut to the border with Abkhazia. From 2016 to 2020, ten large-scale surveys were carried out in different seasons (Table 1). It should be noted that unfavorable weather conditions and the closure of some areas for work did not always make it possible to complete surveys according to the planned scheme.

For hydro-optical measurements, the attenuation coefficient of directional light was measured with a SIPO4 spectral sounder [29], developed in the Department of Optics and Biophysics of the Sea, MHI RAS. BAC was measured in the red region of the spectrum at 625 nm with a vertical resolution of 0.1 m from the surface to the maximum measurement depth. The maximum depth varied from 50 to 200 m on different cruises, depending on the time and weather conditions of the hydro-optical measurements. We calculated TSM concentrations using the empirical ratio $TSM = 1.514 \times BAC(625) - 0.23$, obtained earlier for the northern part of the Black Sea based on the data sets of BAC measurements and determination of the TSM concentration by the gravimetric method, collected at the same stations [28]. Hydrological parameters were measured by the Sea-Bird 911 plus CTD sounding complex; the speed and direction of the currents were measured by the ADCP WORKHORSE-300 kHz current profiler.

To assess the connection of the TSM spatial distributions to thermohaline parameters and their change with depth, we calculated the linear correlation coefficients of TSM versus temperature, salinity, and density for all stations with a vertical step of 1 meter. In addition, we determined a linear correlation between depths of TSM maxima and various thermohaline isosurfaces: the lower boundary of the upper mixed layer, the transition layer, the cold intermediate layer, the boundaries of the redox zone, the upper boundary of the hydrogen sulfide zone, determined by the position of the isopycnal at 16.2 cond. units.

3. Results

An analysis of the TSM horizontal distributions in the surface layer revealed general patterns related to the hydrological structure peculiarities. Within the polygons, there are several areas with TSM extreme values, the appearance of which is associated with the centers of various water masses formation. On majority

Table 1

Cruises of the R/V *Professor Vodyanitsky*, in which measurements of the light beam attenuation coefficient were carried out

Cruise, No	Date	Number of stations
87	30.06–20.07.2016	106
89	16.11–05.12.2016	112
94	22.04–06.05.2017	104
95	14.06–04.07.2017	113
98	14.11–28.11.2017	90
101	14–27.12.2017	62
102	09.06–01.07.2018	122
103	28.08–20.09.2018	147
106	18.04–13.05.2019	142
115	27.11–16.12.2020	76
Total number of stations with BAC measurements		1102

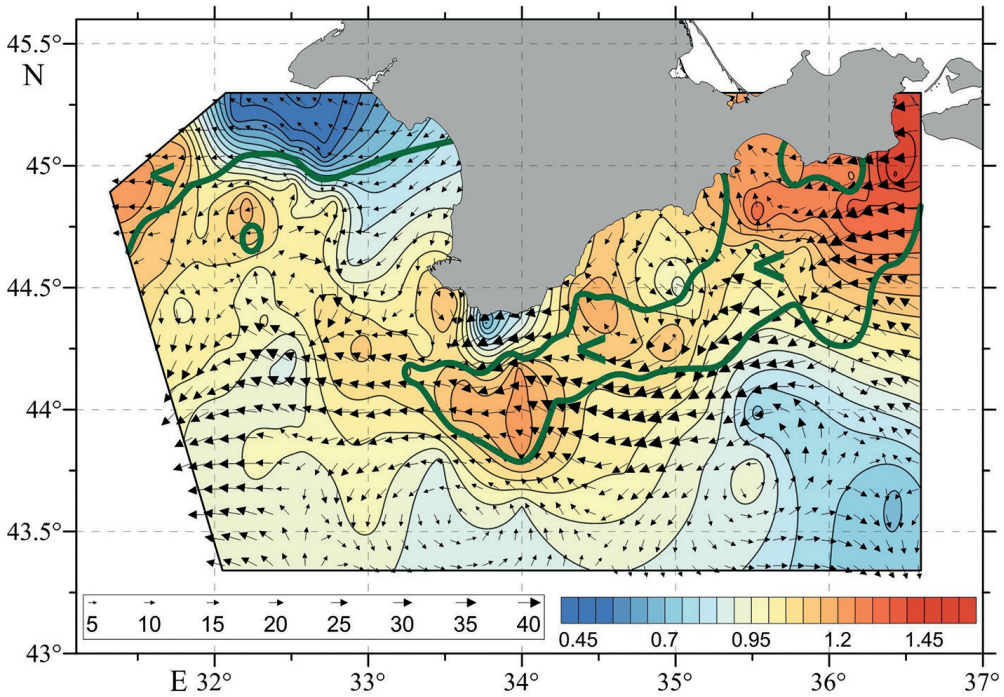

Fig. 1. Distributions of TSM concentration (mg/l) in the surface layer and vectors of instrumentally measured currents (cm/s) at horizon of 25 m during the summer 2017 survey. The position of the 18.1 ‰ isohaline is shown in green

cruises, regardless of the year and season, there were areas with increased TSM values to the south of the Kerch Strait and the Kerch Peninsula. Higher turbidity is associated with the outflow of more turbid and freshened Azov Sea waters through the Kerch Strait. Using the TSM concentration distribution in the summer of 2017 as an example (Fig. 1), it is evident that the area of increased TSM values spread along a vast freshened zone with salinity below 18.1 ‰, formed by the Azov Sea waters. According to the current velocity in situ measurements, these waters propagate westerly with the Rim Current along the Crimean coast. The outflow of the Azov Sea waters with an increased TSM concentration and low salinity from the Kerch Strait and their spread to the west is well reflected in the suspended matter distributions and thermohaline parameters obtained from MODIS/Aqua scanners [30], and the climate array of hydrological measurements of the BOD of MHI [31].

Another region of high TSM values occurs in the eastern part of the Black Sea along the coast of the Caucasus. It was formed by a transfer of muddy and fresh waters of the flows of the Rioni, Enguri and other smaller rivers, such as the Nechepsukho, Ashe, Shakhe, Sochi, and Mzymta, to the northwest by the alongshore branch of Rim Current to the northwest (Fig. 2). Because of water circulation peculiarities, patches of high TSM values were occasionally traced beyond the Caucasian coast in the open sea. Thus, according to the autumn cruise data from August 28 to September 18, 2018, in the open part of the polygon, approximately between 36° and 37°E, 43.5° and 44.5°N, an extensive patch of elevated TSM values were observed (Fig. 2). According to in-situ velocity measurements, this site was located on the northwestern periphery of the large-scale Eastern cyclonic gyre and originated from the thrust of more turbid waters by the Rim Current branch from the coast of the Caucasus to the open sea.

According to the summer cruise, in the period between June 9—July 1, 2018, in the Tuapse area, a maximum TSM concentration was observed, associated with a local source of freshened and turbid waters here (Fig. 3). These waters did not follow the Caucasian coast but propagated from the coast to the deep part (Fig. 3). This can be explained by the alongshore flow decrease of the Rim Current in the eastern part of the polygon recorded by instrumental measurements. At the same time, an anticyclonic eddy formed between Novorossiysk and Tuapse, along the east periphery of which freshened and more turbid waters entered the open deep-water part of the polygon (Fig. 3).

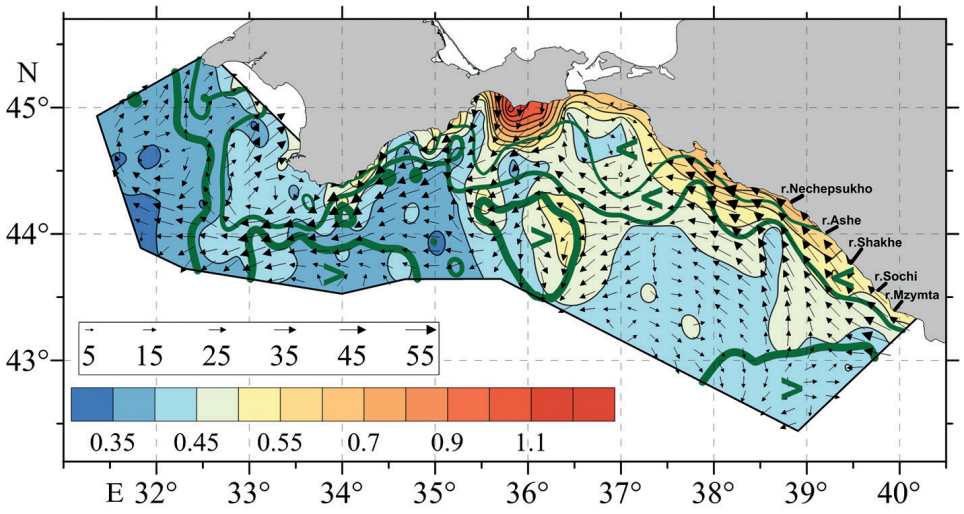

Fig. 2. Distributions of TSM concentration (mg/l) in the surface layer and vectors of instrumentally measured currents (cm/s) at horizon of 25 m during the autumn 2018 survey. Green color shows the position of isochalines 17.85 ‰ (thin line), 18.05 ‰ (middle line), 18.25 ‰ (thick line)

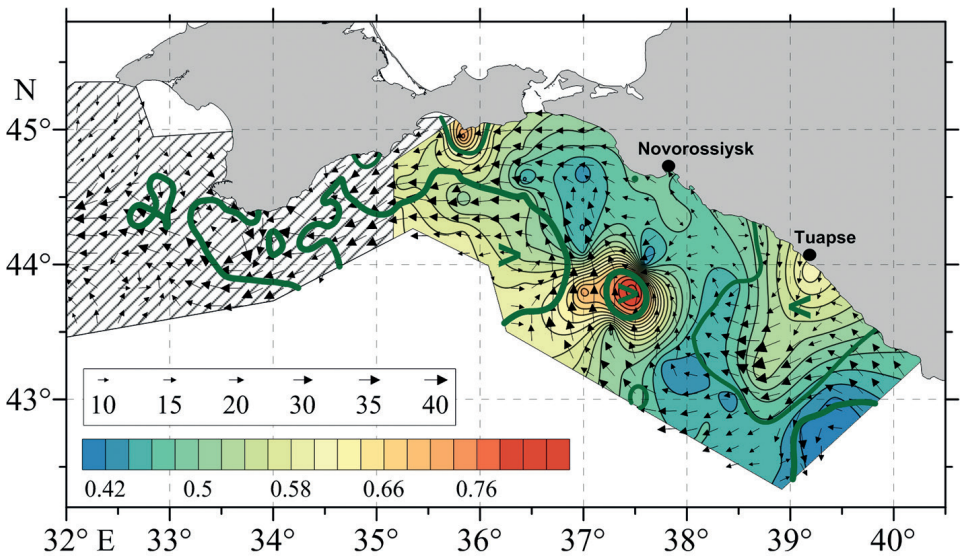

Fig. 3. Distributions of TSM concentration (mg/l) in the surface layer and vectors of instrumentally measured currents (cm/s) at horizon of 25 m during the summer 2018 survey. The positions of isochalines 17,9 ‰ (thin line) and 18,15 ‰ (thick line) are shown in green. The area where hydrooptical measurements were not taken is shaded

In the northwestern part of the polygons, during spring-summer cruises, one more area of increased TSM values was registered (Fig. 1; Fig. 4, *a*). In this area, as a rule, waters of low salinity were observed, which penetrated the survey area from the northwestern shelf (Fig. 1; Fig. 4, *a*). Shelf waters are characterized by maximum turbidity and minimum salinity due to the runoff of Dnieper, Southern Bug, Dniester, and Danube rivers [7, 9–12, 21, 22].

In addition to the above areas of high TSM concentrations, in the deep part of the polygon, local areas of turbid waters can be traced. Apparently, the existence of these regions is not associated with river runoff or advection of coastal waters into the open sea. The occurrence of such areas can be explained by vertical circulation peculiarities in the cyclonic gyres and meanders. So, for example, according to the summer and

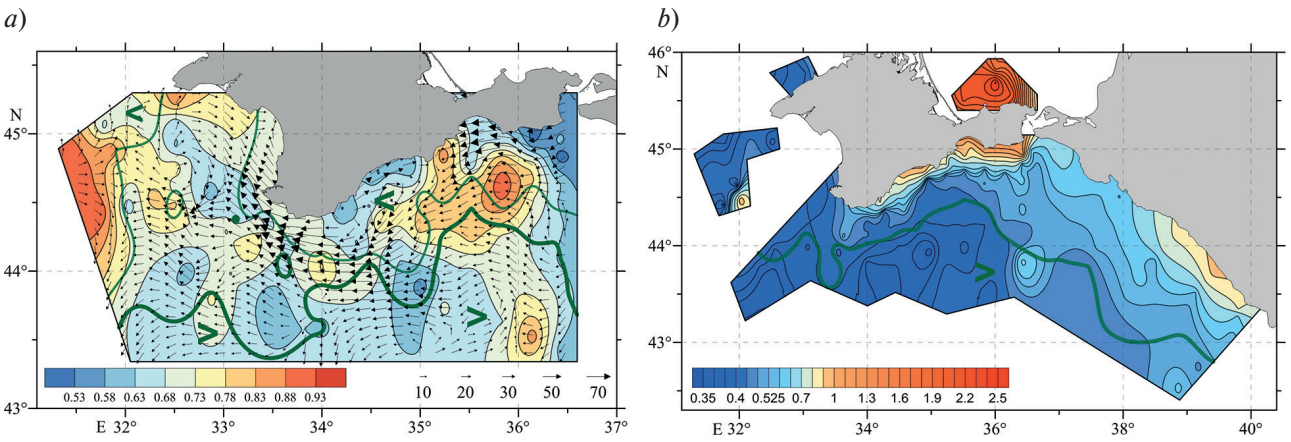

Fig. 4. Distributions of TSM concentration (mg/l) in the surface layer and vectors of instrumentally measured currents (cm/s) at horizon of 25 m during the summer 2016 survey (*a*) and TSM concentration during spring 2019 survey (*b*). Green color shows the position of isochalines 17,9 ‰ (thin line) and 18,15 ‰ (thick line) (*a*), 18,45 ‰ (thick line) (*b*)

autumn surveys in 2018, in the southern part of the polygons, areas of high TSM values were observed located on the peripheries of cyclonic meanders (Figs. 2, 3). In contrast to coastal waters with high turbidity and low salinity, waters with high TSM concentrations in the zones of these meanders were characterized by an increase in surface salinity above 18.15 ‰ in summer and 18.25 ‰ in autumn (Fig. 2, 3). This increase in turbidity and salinity is associated with the rise of more saline subsurface waters and a subsurface maximum of TSM concentration, which leads to elevated TSM and salinity near the surface. TSM maximum depth distribution varied from shallow 5–10 m in the regions of high surface TSM to deepened 15–25 m in the surrounding waters [25].

In general, according to the data of all cruises in the deep-waters, the TSM concentration decreased with distance from the coastal sources of turbid waters, while salinity, as a rule, increased (Fig. 4).

4. Discussion

Quasi-synchronous measurements of the TSM concentration and hydrological parameters during surveys provided data for some statistical estimates of the identified features of a relationship between the spatial structure of hydrological fields and the TSM field on the surface and for analysis of the variability of this relationship with depth. An analysis of the horizontal distributions of the TSM concentrations and thermohaline parameters, as well as the linear relationship coefficients between these distributions with the increments of 1 m in depth, showed that within the upper upper mixed layer (UML) there was significant negative linear correlation between the values of the TSM versus temperature and salinity at each horizon. The correlation between TSM and density was positive [23, 26]. Thus, colder and less saline waters tended to have increased turbidity due to the intense growth of organisms in colder waters, confined mainly to the open parts of the sea and upwellings. In less saline waters, an increase in TSM concentration occurred predominantly in coastal areas, where there is a significant input of river runoff enriched with particulate matter of terrigenous origin.

The UML thickness in the TSM field significantly depended on the season (Fig. 5, *a*) and, as a rule, coincided with the UML thickness in the fields of thermohaline parameters (Fig. 5, *b*, *d*, *f*). From late autumn to spring, a well-developed UML with a thickness of up to 50 m was observed; in summer and early autumn, the UML thickness did not exceed 5–10 m. Deeper than the UML, a subsurface maximum of TSM concentration was traced, most prominent in summer and autumn (Fig. 5, *a*). The depth of this maximum was 10–13 m in summer, increased to 18–22 m in early autumn, and up to 25 m at the end of autumn. The distributions of vertical gradients of temperature (TVG), salinity (SVG), and density (σ_tVG) (Fig. 5, *c*, *e*, *g*) showed that the depth of the subsurface maximum of TSM concentration coincided well with the depth

of the maximum values (in absolute value) of vertical temperature and density gradients (Fig. 5, *a*, *c*, *g*). In general, a strong linear relationship exists between the depths of the TSM subsurface maxima and the maxima of the TVG and σ_tVG in the summer-autumn season (Table 2). In addition, it was found that the thickness of the subsurface layer with high TSM concentrations, more than 1.5 times higher than the TSM values in the overlying and underlying layers, depends on the absolute value of the vertical temperature gradient. In areas of TSM maxima, the layer thickness with a high content of total suspended matter decreased by almost an order of magnitude compared to areas where the temperature gradient was weak. A significant linear correlation was obtained for the thickness of the layer with the maximum TSM concentration and the value of the maximum TVG (Fig. 6).

During winter and spring cruises, the vertical stratification of the TSM concentration in the upper 60-m layer was weak, and the subsurface maximum was practically undetectable. Directly in the surface layer up to 5 m thick, weak extrema of different signs were observed in the TSM structure, which resulted from the influence of synoptic atmospheric processes on the redistribution of surface waters with different TSM concentrations (Fig. 5, *a*).

Below the subsurface maximum, the TSM concentration gradually decreased (Fig. 7, *a*). The cruises' results show an intermediate TSM minimum within a 75–120 m layer, and its depth varies from 75–95 m in late autumn, winter and spring to 100–117 m in summer and early autumn. The vertical temperature distribution (Fig. 7, *b*) shows that this TSM minimum laid below the depth of the temperature minimum (the core

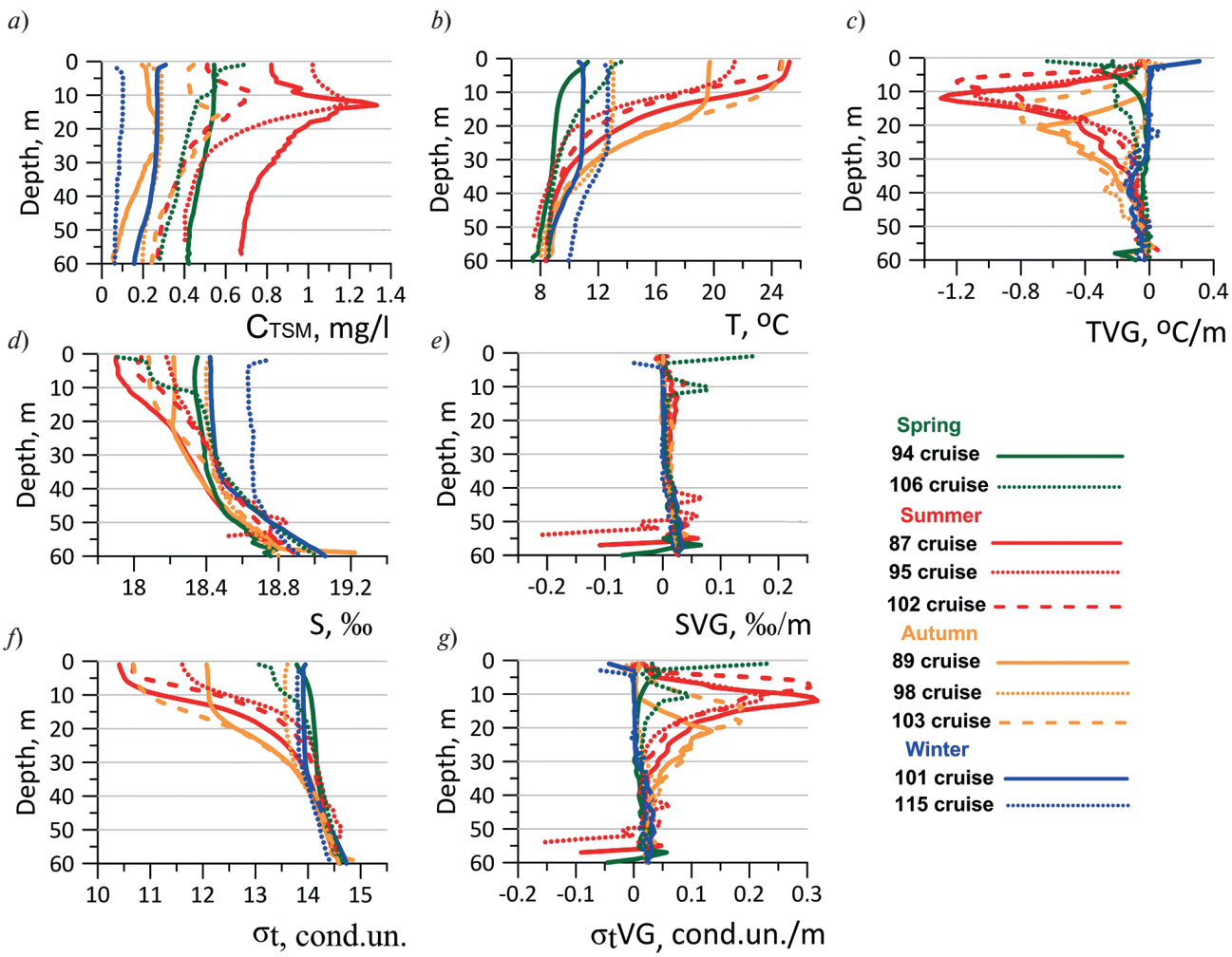

Fig. 5. Vertical profiles of TSM concentration (*a*), temperature (*b*) and TVG (*c*), salinity (*d*) and SVG (*e*), density σ_t (*f*) and σ_tVG (*g*) in the 0–60 m layer, averaged over all stations for each survey

Table 2

Values of the linear correlation coefficients R between the depths of occurrence (H) of the subsurface maximum of the C_{TSM} and the maximum of the TVG and σtVG. R values significant at the 95% level are shown in bold

Parameter	Spring		Summer			Autumn			Winter	
	2017	2019	2016	2017	2018	2016	2017	2018	2018	2020
R(HTSMmax — TVGmax)	0.32	**0.94**	**0.91**	**0.65**	**0.9**	**0.82**	0.33	**0.82**	0.1	0.35
R(HTSMmax — σtVGmax)	0.35	**0.95**	**0.91**	**0.65**	**0.74**	**0.79**	0.35	**0.83**	0.1	0.25

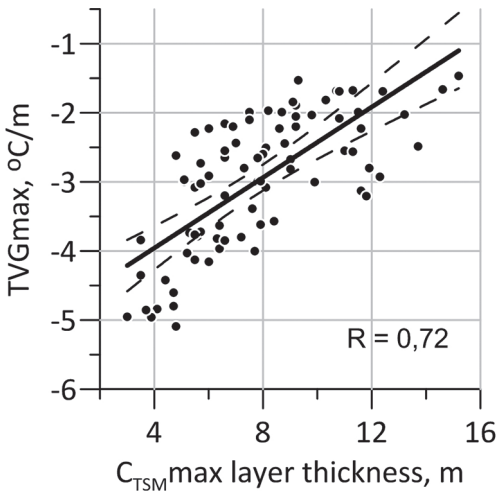

Fig. 6. Correlation between the thickness of the subsurface layer with high TSM concentrations and the value of the maximum temperature vertical gradient according to the data of the summer 2016 survey. Dashed lines are the boundaries of the 95% confidence interval

of the cold intermediate layer (CIL)), which occurred on 70–90 m, and was located in the layer of the main thermocline, halocline, and pycnocline (Fig. 7, *b — d*). In general, a significant linear relationship was found between the depths of the CIL core and the intermediate TSM minimum (Fig. 7, *e*).

Below the intermediate minimum, the TSM concentration increased again. And at depths beneath 100–120 m, several relatively weak TSM extrema were recorded on the vertical profiles averaged over all stations (Fig. 7, *a*). An analysis of the vertical structure of the density field showed that the greatest increase in the content of suspended matter is observed in the layer of isopycnal surfaces 16.15–16.35 cond. units. According to [13], this layer covers the lower boundary of the suboxygen redox zone and the upper layer of the hydrogen sulfide zone, the upper boundary of which is here determined by the position of the isopycnal 16.2 cond. units. The most intense deep maximum of the TSM concentration was well traced during the autumn survey in 2017. On the averaged TSM profile, this maximum was located approximately at a depth of 170 m (Fig. 7, *a*; Fig. 8, *a*), which corresponded to an isopycnal surface of 16.3 cond. units (Fig. 8, *b*), i.e., according to [13], was in the upper part of the hydrogen sulfide zone. An analysis of the depth of occurrence of TSM maximum at each individual station showed that across the survey area it varied in a wide range from 100 to 170 m. The consistency estimates of the spatial distribution of the TSM maxima depths and various isopycnal surfaces with increments of 0.1 cond. unit, corresponding to the suboxygen redox zone (15.5–16.15 cond. units) (Fig. 8, *c*) and the hydrogen sulfide zone (16.2–16.6 cond. units) (Fig. 8, *d — f*) showed that the maximum correlation reaching R ~ 0.936 is observed for the isopycnal depth of 16.3 cond. units. In general, a high level of consistency in the distribution of the TSM maxima depths in the hydrogen sulfide zone with the distribution of the layer of isopycnal surfaces of 16–16.4 cond. units with R values exceeding 0.9 (Fig. 8, *g*) was observed.

5. Conclusion

Detailed hydro-optical surveys with high spatial resolution, performed on the same grid, provided data to clarify the features of horizontal and vertical structures of hydro-optical fields and evaluate their relationship with hydrological characteristics.

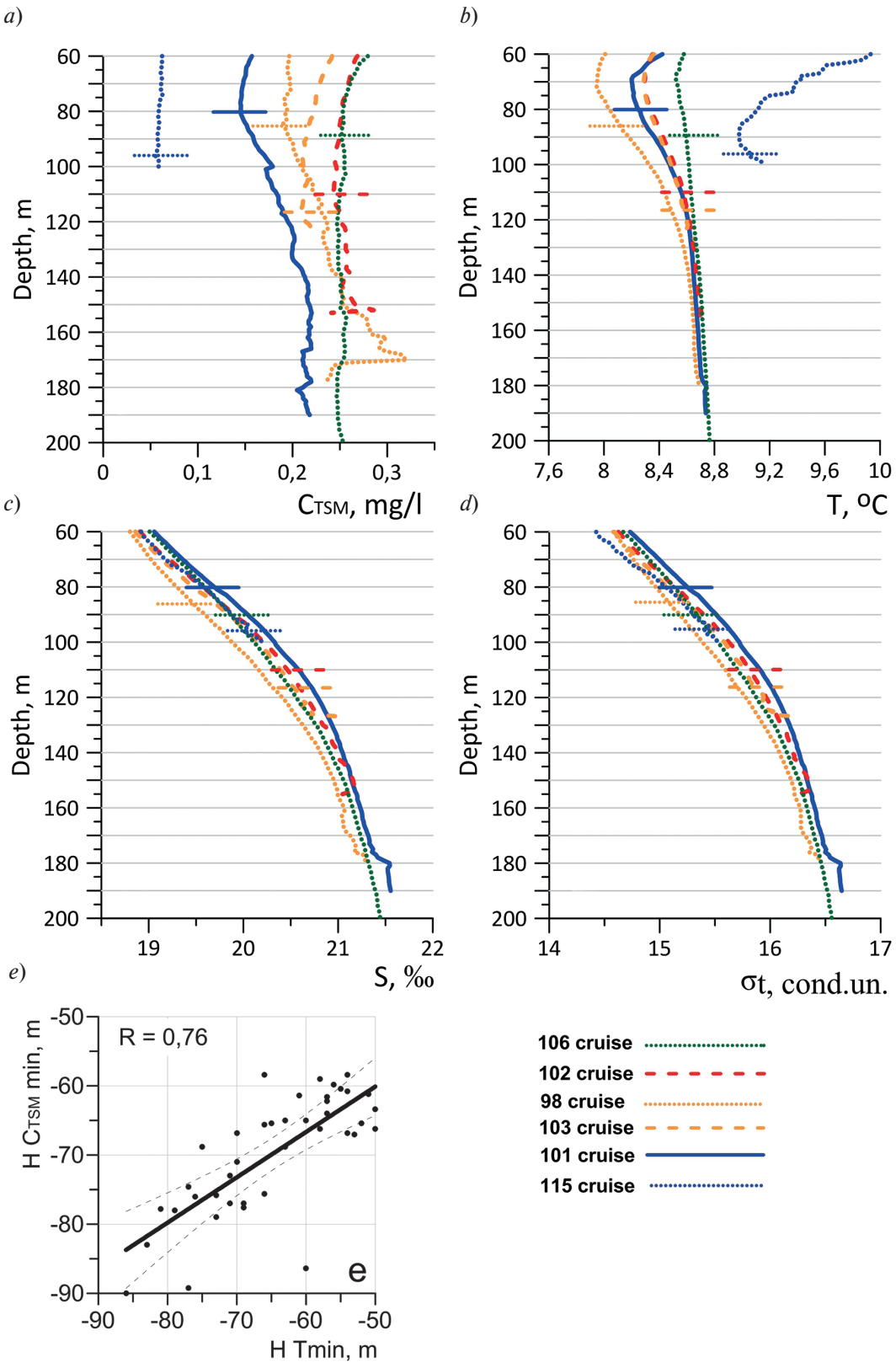

Fig. 7. Vertical profiles of TSM concentration (*a*), temperature (*b*), salinity (*c*) and density (*d*) in the 60–200 m layer, averaged over all stations for each survey, and the correlation between the depths of the CIL core and C_{TSM} intermediate minimum (*e*) according to the data of the winter 2017 survey. The horizontal lines mark the depth of the TSM minimum. Dashed lines are the boundaries of the 95 % confidence interval

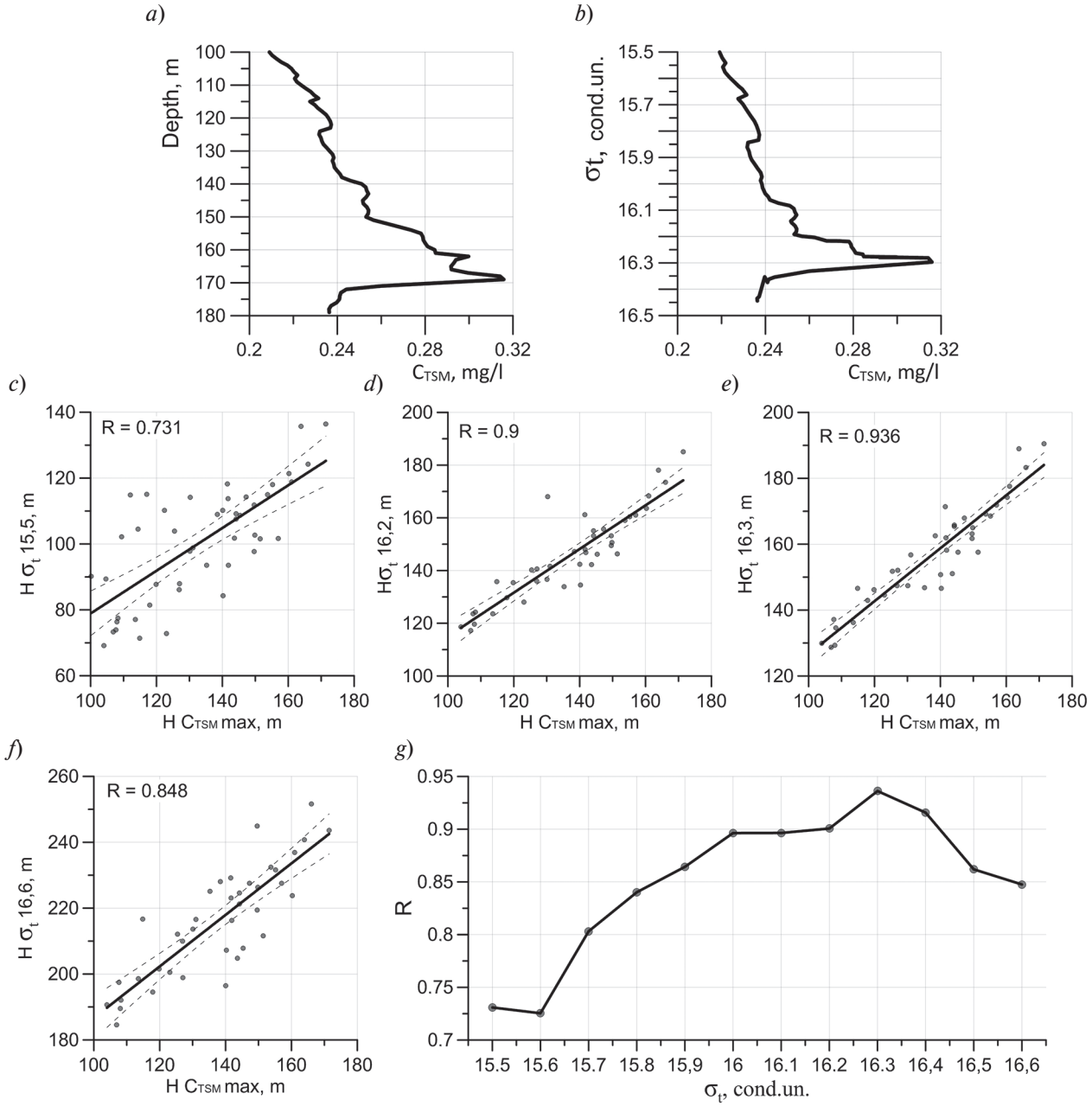

Fig. 8. Averaged over all stations, the C_{TSM} vertical profile in the 100–180 m layer (*a*), dependence of the C_{TSM} values on density (*b*), correlation between the depths of different isopycnes and the C_{TSM} maximum in the suboxygen zone (*c*), at the upper boundary of the hydrogen sulfide zones (*d*), in the hydrogen sulfide zone (*e*,*f*), change of the correlation coefficient R between the depths of the C_{TSM} maximum and different isopycnes (*g*) according to the data of the autumn 2017 survey. Dashed lines are the boundaries of the 95 % confidence interval

It is shown that the sources of increased concentration of total suspended matter in the surface layer of the northern part of the Black Sea are low-salinity and turbid waters coming from the Kerch Strait; the waters of the Rioni, Enguri, and other rivers in the east of the study region; and the freshened waters of the Dnieper, Dniester and Danube penetrating survey area from the northwestern shelf.

In the deep part of the survey areas, local patches of turbid waters can occur, associated with the peculiarities of vertical circulation in the cyclonic gyres and meanders of the Rim Current. Unlike coastal waters with increased turbidity and low salinity, waters with increased TSM concentration in the zones of these meanders were characterized by high surface salinity.

It was found that within the upper mixed layer, at each horizon, a significant negative linear correlation was observed between the TSM values and temperature, TSM and salinity, and a positive correlation between the values of TSM and density, i.e. colder and less saline, as well as denser waters were characterized by increased turbidity.

It is shown that the thickness of the UML in the TSM field, as a rule, coincided with the thickness of the UML of thermohaline parameters. Deeper than the UML, the main TSM maximum was registered, most prominent in summer and autumn. The depth of TSM maximum coincided with the depth of the maximum values (in absolute value) of the vertical gradients of temperature and density. The thickness of the subsurface layer with high TSM concentrations, more than 1.5 times higher than the TSM values in the overlying and underlying layers, was linked to the absolute value of the vertical temperature gradient. In areas where the TSM maximum was observed, the thickness of the layer with a high content of total suspended matter decreased by almost an order of magnitude compared to areas where the temperature gradient was weak.

Below the depth of the cold intermediate layer core, in the layer of the main thermocline, halocline, and pycnocline, an intermediate TSM minimum was registered. Beneath the intermediate minimum, the concentration of TSM increased again. At depths below 120–130 m one more TSM maximum occurred, located in the upper layer of the hydrogen sulfide zone. The spatial distribution of the depth of occurrence of this maximum is most clearly consistent with the distribution of the depth of the isopycnal 16.3 cond. units.

6. Acknowledgments

The authors express their deep gratitude for valuable methodological advice during the discussion of the article to the senior research scientist of the Department of remote research methods, FSBSI FRC MHI, A.N. Morozov.

7. Funding

The work was carried out within the framework of the **FSBSI FRC MHI** State Orders No. 0555-2021-0003 (Operational oceanology) and № 0555-2021-0004 (Oceanological processes).

References

1. *Israel Yu.A.*, *Tsyban A.V.* Anthropogenic ecology of the ocean. *Moskva*, *Flinta Nauka*, 2009. 520 p. (in Russian).
2. *Ivanov V.A.*, *Katunina E.V.*, *Sovga E.E.* Assessments of anthropogenic impacts on the ecosystem of the waters of the Heraklean Peninsula in the vicinity of deep drains. *Processes in GeoMedia*. 2016, 1(5), 62–68 (in Russian).
3. *Bondur V.G.*, *Kiler R.N.*, *Starchenkov S.A.*, *Rybakova N.I.* Monitoring of the pollution of the ocean coastal waters areas using space multispectral high resolution imagery. *Issledovanie Zemli iz Kosmosa*. 2006, 6, 42–49 (in Russian).
4. *Volpe V.*, *Silvestri S.*, *Marani M.* Remote sensing retrieval of suspended sediment concentration in shallow waters. *Remote Sensing of Environment*. 2011, 115, 1, 44–54. doi:10.1016/j.rse.2010.07.013
5. *Xiaolong Yu.*, *Zhongping L.*, *Fang S.*, *Menghua W.*, *Jianwei W.*, *Lide J.*, *Zhehai S.* An empirical algorithm to seamlessly retrieve the concentration of suspended particulate matter from water color across ocean to turbid river mouths. *Remote Sensing of Environment*. 2019, 235, 111491. doi:10.1016/j.rse.2019.111491
6. *Eisma D.* Suspended matter in the aquatic environment. Berlin, Heidelberg: Springer-Verlag. 1993, 315 p. doi:10.1007/978-3-642-77722-6
7. *Man'kovskiy V.I.* Optical structure of the Black Sea waters and patterns of its formation. *Gidrofizicheskie i Gidrohimicheskie Issledovaniya Chernogo Morya. Sevastopol, MGI ANU*. 1992, 7–27 (in Russian).
8. *Man'kovskiy V.I.*, *Solov'ev M.V.* Relationship between the radiation attenuation index and the concentration of suspended matter in the Black Sea waters. *Morskoy Gidrofizicheckiy Zhurnal*. 2003, 2, 60–65 (in Russian).
9. *Man'kovskiy V.I.*, *Man'kovskaya E.V.*, *Solov'ev M.V.* Hydro-optical characteristics of the Black Sea. *Reference book. Sevastopol', MGI NAN Ukrainy*, 2009. 41 p. (in Russian).
10. *Kukushkin A.S.*, *Agafonov E.A.*, *Prohorenko Yu.A.* Distribution of the light beam attenuation coefficient in the surface coastal waters of the Black Sea. *Morskoy Gidrofizicheckiy Zhurnal*. 2006, 5, 30–43 (in Russian).
11. *Kukushkin A.S.* Spatial and temporal variability of the water transparency distribution in the north-western Black Sea. *Optika Atmosfery i Okeana*. 2017, 30(9), 750–762 (in Russian). doi:10.15372/AOO20170904
12. *Man'kovskiy V.I.* Optical characteristics of the coastal waters of the Black Sea coast of Ukraine. *Ekologicheskaya Bezopasnost' Pribrezhnyh i Shel'fovyh Zon i Kompleksnoe Ispol'zovanie Resursov Shel'fa*. 1999, 149–152 (in Russian).
13. *Yakushev E.V.*, *Chasovnikov V.K.*, *Murray J.W.*, *Pakhomova S.V.*, *Podymov O.I.*, *Stunzhas P.A.* Vertical hydro-chemical structure of the Black Sea / Eds. Kostianoy A.G., Kosarev A.N. The Black Sea Environment. The Handbook of Environmental Chemistry. Berlin, Heidelberg: Springer. Vol. 5Q. 2007. P. 277–307. doi:10.1007/698_5_088

14. *Man'kovskiy V.I.* A deep layer of increased concentration of suspended matter and its relationship with the circulation and structure of water masses. *Issledovaniya Mezhvedomstvennoy Ekspedicii v Severo-zapadnoy Atlantike. Sevastopol', MGI AN USSR*, 1969. P. 83–88 (in Russian).
15. *Neujmin G.G.* Stable deep-water suspension layer in the Black Sea. *Morskie Gidrofizicheskie Issledovaniya*. 1970, 1, 178–191 (in Russian).
16. *Neujmin G.G.* Distribution of suspended matter in the deep areas of the Black Sea. *Fizika Atmosfery i Okeana*. 1965, 1(11), 1190–1195 (in Russian).
17. *Sovga E.E.*, *Man'kovskiy V.I.*, *Prohorenko Yu.A.*, *Chepurnova E.A.* Nature of the turbidity deep layer in the Black Sea. *Doklady Akademii nauk Ukrainskoy SSR. Seriya B: Geologicheskie, himicheskie i biologicheskie nauki*. 1987, 6, 32 (in Russian).
18. *Prohorenko Yu.A.*, *Krasheninnikov B.N.*, *Agafonov E.A.*, *Basharin V.A.* Experimental studies of the turbidity deep layer in the Black Sea. *Morskoy Gidrofizicheckiy Zhurnal*. 1993, 2, 57–63 (in Russian).
19. *Man'kovskiy V.I.*, *Zemlyanaya L.A.* Distribution over the water area and seasonal variability of the turbidity deep layer in the Black Sea. *Morskoy Gidrofizicheckiy Zhurnal*. 1987, 6, 51–53 (in Russian).
20. *Man'kovskiy V.I.* Features of the vertical distribution of the radiation attenuation coefficient in the short-wave and long-wave parts of the spectrum in the deep layers of the hydrogen sulfide zone and in the bottom layer of the Black Sea. *Morskoy Gidrofizicheckiy Zhurnal*. 2003, 3, 63–67 (in Russian).
21. *Agafonov E.A.*, *Kukushkin A.S.*, *Prohorenko Yu.A.* Features of the formation of surface water transparency on the shelf of the northern regions of the Black Sea. *Morskoy Gidrofizicheckiy Zhurnal*. 2002, 2, 65–67 (in Russian).
22. *Man'kovskiy V.I.* Optical characteristics of waters in the eastern part of the northwestern shelf of the Black Sea in the spring. *Morskoy Gidrofizicheckiy Zhurnal*. 2012, 4, 61–68 (in Russian).
23. *Latushkin A.A.*, *Artamonov Yu.V.*, *Fedirko A.V.*, *Martynov O.V.*, *Alekseev D.V.* Peculiarities of the suspended matter distribution received by the optical measurements in the photic layer of the north part of the Black Sea in the summer period of 2016. *Proceedings SPIE*, *23rd International Symposium on Atmospheric and Ocean Optics*: *Atmospheric Physics*, 1046634 (2017). doi: 10.1117/12.2286444
24. *Latushkin A.A., Artamonov Yu.V., Fedirko A.V., Korchemkina E.N., Skripaleva E.A., Khurchak A.P.* Hydro-optical structure of the Black Sea active water layer in the spring-summer period of 2017. *Proceedings SPIE10833*, *24th International Symposium on Atmospheric and Ocean Optics: Atmospheric Physics*, 2018. 108333V. doi:10.1117/12.2503874
25. *Latushkin A.A.*, *Artamonov Yu.V.*, *Fedirko A.V.*, *Skripaleva E.A.*, *Kudinov O.B.* Features of the waters hydro-optical structure in the northern part of the Black Sea according to field measurements in 2018. *Proceedings of X Anniversary All-Russian Conference* "*Current Problems in Optics of Natural Waters*" (*ONW 2019*). *St. Peterburg*, 2019, 120–124 (in Russian).
26. *Latushkin A.A.*, *Artamonov Yu.V.*, *Fedirko A.V.*, *Skripaleva E.A.*, *Kudinov O.B.* Spatial structure of the total suspended matter concentrations in the northern Black Sea in autumn 2018 according to contact observations. *Proceedings SPIE*11208, 25th *International Symposium on Atmospheric and Ocean Optics: Atmospheric Physics*, 2019. 112084U. doi:10.1117/12.2540798
27. *Latushkin A.A.*, *Artamonov Yu.V.*, *Skripaleva E.A.*, *Fedirko A.V.*, *Kudinov O.B.* Spatial features of the hydro-optical waters structure in the northern part of the Black Sea in spring 2019 according to contact measurements on R/V *Professor Vodyanitsky*. Proceedings SPIE11560, 26th International Symposium on Atmospheric and Ocean Optics: Atmospheric Physics, 2020. 115602R. doi:10.1117/12.2574281
28. *Klyuvitkin A.A.*, *Garmashov A.V.*, *Latushkin A.A.*, *Orekhova N.A.*, *Kochenkova A.I.*, *Malafeev G.V.* Comprehensive Studies of the Black Sea during the Cruise 101 of the R/V Professor Vodyanitsky. *Oceanology*. 2019, 59, 2, 287–289. doi:10.1134/S0001437019020097
29. *Latushkin A.A.* Multi-channel beam attenation coefficient meter for oceanographic sub-satellite research. *Upravlenie i Mekhanotronnye Sistemy*. 2013, 231–236 (in Russian).
30. *Aleskerova A.A.*, *Kubryakov A.A.*, *Goryachkin Yu.N.*, *Stanichny S.V.* Propagation of waters from the Kerch Strait in the Black Sea. *Physical Oceanography*. 2017, 6, 47–57. doi:10.22449/1573-160X-2017-6-47-57
31. *Artamonov Yu.V.*, *Latushkin A.A.*, *Skripaleva E.A.*, *Fedirko A.V.* Rim Current manifestation in the climatic fields of hydro-optical and hydrological characteristics at the coast of Crimea. *Proceedings SPIE1*1208, *25th International Symposium on Atmospheric and Ocean Optics: Atmospheric Physics*, 2019. C3–112084X. doi:10.1117/12.2540803

Литература

1. *Израэль Ю.А.*, *Цыбань А.В.* Антропогенная экология океана. М.: Флинта Наука, 2009. 520 с.
2. *Иванов В.А.*, *Катунина Е.В., Совга Е.Е.* Оценки антропогенных воздействий на экосистему акватории Гераклейского полуострова в районе расположения глубинных стоков // Процессы в геосредах. 2016. Т. 1, № 5. С. 62–68.
3. *Бондур В.Г.*, *Килер Р.Н.*, *Старченков С.А.*, *Рыбакова Н.И.* Мониторинг загрязнений прибрежных акваторий с использованием многоспектральных спутниковых изображений высокого пространственного разрешения // Исследование Земли из космоса. 2006. № 6. С. 42–49.

4. *Volpe V.*, *Silvestri S.*, *Marani M.* Remote sensing retrieval of suspended sediment concentration in shallow waters // Remote Sensing of Environment. 2011. Vol. 115, Iss. 1. P. 44–54. doi:10.1016/j.rse.2010.07.013
5. *Xiaolong Yu*, *Zhongping L.*, *Fang S.*, *Menghua W.*, *Jianwei W.*, *Lide J.*, *Zhehai S.* An empirical algorithm to seamlessly retrieve the concentration of suspended particulate matter from water color across ocean to turbid river mouths // Remote Sensing of Environment. 2019. Vol. 235. doi:10.1016/j.rse.2019.111491
6. *Eisma D.* Suspended matter in the aquatic environment. Berlin, Heidelberg: Springer-Verlag. 1993, 315 p. doi:10.1007/978-3-642-77722-6
7. *Маньковский В.И.* Оптическая структура вод Черного моря и закономерности ее формирования // Гидрофизические и гидрохимические исследования Черного моря. Севастополь: МГИ АНУ, 1992. С. 7–27.
8. *Маньковский В.И.*, *Соловьев М.В.* Связь показателя ослабления излучения с концентрацией взвеси в водах Черного моря // Морской гидрофизический журнал. 2003. № 2. С. 60–65.
9. *Маньковский В.И.*, *Маньковская Е.В.*, *Соловьев М.В.* Гидрооптические характеристики Черного моря. Справочник. Севастополь: МГИ НАН Украины, 2009. 41 с.
10. *Кукушкин А.С.*, *Агафонов Е.А.*, *Прохоренко Ю.А.* Распределение показателя ослабления направленного света в поверхностных прибрежных водах Черного моря // Морской гидрофизический журнал. 2006. № 5. С. 30–43.
11. *Кукушкин А.С.* Пространственно-временная изменчивость распределения прозрачности вод в северо-западной части Черного моря // Оптика атмосферы и океана. 2017. Т. 30, № 9. С. 750–762. doi:10.15372/AOO20170904
12. *Маньковский В.И.* Оптические характеристики прибрежных вод Черноморского побережья Украины // Экологическая безопасность прибрежных и шельфовых зон и комплексное использование ресурсов шельфа. 1999. С. 149–152
13. *Yakushev E.V.*, *Chasovnikov V.K.*, *Murray J.W.*, *Pakhomova S.V.*, *Podymov O.I.*, *Stunzhas P.A.* Vertical hydro-chemical structure of the Black Sea / Eds. Kostianoy A.G., Kosarev A.N. The Black Sea Environment. The Handbook of Environmental Chemistry. Berlin, Heidelberg: Springer. Vol. 5Q. 2007. P. 277–307. doi:10.1007/698_5_088
14. *Маньковский В.И.* Глубинный слой повышенной концентрации взвеси и его связь с циркуляцией и структурой водных масс // Исследования межведомственной экспедиции в северо-западной Атлантике. Севастополь: МГИ АН УССР. 1969. С. 83–88.
15. *Неуймин Г.Г.* Стабильный глубоководный слой взвеси в Черном море // Морские гидрофизические исследования. Севастополь: МГИ АН УССР. 1970. № 1. С. 178–191.
16. *Неуймин Г.Г.* Распределение взвеси в глубинных областях Черного моря // Физика атмосферы и океана. 1965. Т. 1, № 11. С. 1190–1195.
17. *Совга Е.Е.*, *Маньковский В.И.*, *Прохоренко Ю.А.*, *Чепурнова Э.А.* Природа глубинного мутного слоя в Черном море // Доклады Академии наук Украинской ССР. Серия Б: Геологические, химические и биологические науки. 1987. № 6. С. 32.
18. *Прохоренко Ю.А.*, *Крашенинников Б.Н.*, *Агафонов Е.А.*, *Башарин В.А.* Экспериментальные исследования глубинного слоя мутности в Черном море // Морской гидрофизический журнал. 1993. № 2. С. 57–63.
19. *Маньковский В.И.*, *Земляная Л.А.* Распределение по акватории и сезонная изменчивость глубинного мутного слоя в Черном море // Морской гидрофизический журнал. 1987. № 6. С. 51–53.
20. *Маньковский В.И.* Особенности вертикального распределения показателя ослабления излучения в коротковолновом и длинноволновом участках спектра в глубинных слоях сероводородной зоны и в придонном слое Черного моря // Морской гидрофизический журнал. 2003. № 3. С. 63–67.
21. *Агафонов Е.А.*, *Кукушкин А.С.*, *Прохоренко Ю.А.* Особенности формирования прозрачности поверхностных вод на шельфе северных районов Черного моря // Морской гидрофизический журнал. 2002. № 2. С. 65–67.
22. *Маньковский В.И.* Оптические характеристики вод восточной части северо-западного шельфа Черного моря в весенний период // Морской гидрофизический журнал. 2012. № 4. С. 61–68.
23. *Latushkin A.A.*, *Artamonov Yu.V.*, *Fedirko A.V.*, *Martynov O.V.*, *Alekseev D.V.* Peculiarities of the suspended matter distribution received by the optical measurements in the photic layer of the north part of the Black Sea in the summer period of 2016 // Proceedings SPIE, 23rd International Symposium on Atmospheric and Ocean Optics: Atmospheric Physics, 1046634 (2017). doi: 10.1117/12.2286444
24. *Latushkin A.A.*, *Artamonov Yu.V.*, *Fedirko A.V.*, *Korchemkina E.N.*, *Skripaleva E.A.*, *Khurchak A.P.* Hydro-optical structure of the Black Sea active water layer in the spring-summer period of 2017 // Proceedings SPIE10833, 24th International Symposium on Atmospheric and Ocean Optics: Atmospheric Physics, 2018. 108333V. doi:10.1117/12.2503874
25. *Латушкин А.А.*, *Артамонов Ю.В.*, *Федирко А.В.*, *Скрипалева Е.А.*, *Кудинов О.Б.* Особенности гидрооптической структуры вод в северной части Черного моря по данным натурных измерений в 2018 г. // Труды X-ой Всероссийской конференции с международным участием «Современные проблемы оптики естественных вод» (ONW 2019). Санкт-Петербург, 2019. С. 120–124.

26. *Latushkin A.A.*, *Artamonov Yu.V.*, *Fedirko A.V.*, *Skripaleva E.A.*, *Kudinov O.B.* Spatial structure of the total suspended matter concentrations in the northern Black Sea in autumn 2018 according to contact observations // Proceedings SPIE11208, 25th International Symposium on Atmospheric and Ocean Optics: Atmospheric Physics, 2019. 112084U. doi:10.1117/12.2540798
27. *Latushkin A.A.*, *Artamonov Yu.V.*, *Skripaleva E.A.*, *Fedirko A.V.*, *Kudinov O.B.* Spatial features of the hydro-optical waters structure in the northern part of the Black Sea in spring 2019 according to contact measurements on R/V *Professor Vodyanitsky* // Proceedings SPIE11560, 26th International Symposium on Atmospheric and Ocean Optics: Atmospheric Physics, 2020. 115602R. doi:10.1117/12.2574281
28. *Клювиткин А.А.*, *Гармашов А.В.*, *Латушкин А.А.*, *Орехова Н.А.*, *Коченкова А.И.*, *Малафеев Г.В.* Комплексные исследования Черного моря в 101-М рейсе научно-исследовательского судна «Профессор Водяницкий» // Океанология. 2019. Т. 59, № 2. С. 315–318. doi:10.31857/S0030-1574592315-318
29. *Латушкин А.А.* Многоканальный измеритель коэффициента ослабления света для проведения океанографических подспутниковых исследований // Управление и механотронные системы. Севастополь: МГИ НАН Украины, 2013. С. 231–236.
30. *Алескерова А.А.*, *Кубряков А.А.*, *Горячкин Ю.Н.*, *Станичный С.В.* Распространение вод из Керченского пролива в Черное море // Морской гидрофизический журнал. 2017. № 6. С. 53–64. doi:10.22449/0233-7584-2017-6-53-64
31. *Artamonov Yu.V.*, *Latushkin A.A.*, *Skripaleva E.A.*, *Fedirko A.V.* Rim Current manifestation in the climatic fields of hydro-optical and hydrological characteristics at the coast of Crimea // Proceedings SPIE11208, 25th International Symposium on Atmospheric and Ocean Optics: Atmospheric Physics, 2019. C3–112084X. doi:10.1117/12.2540803